



AFRL-AFOSR-JP-TR-2023-0071

Multifunctional Behavior of Fe-Doped Titanate-Based High-Entropy Perovskite Oxides

**NATTHAPHON RAENGTION
CHULALONGKORN UNIVERSITY
254 PHAYATHAI ROAD
PATHUM WAN, BANGKOK, 10330
THA**

**03/22/2023
Final Technical Report**

DISTRIBUTION A: Distribution approved for public release.

Air Force Research Laboratory
Air Force Office of Scientific Research
Asian Office of Aerospace Research and Development
Unit 45002, APO AP 96338-5002

REPORT DOCUMENTATION PAGE

PLEASE DO NOT RETURN YOUR FORM TO THE ABOVE ORGANIZATION.

1. REPORT DATE 20230322	2. REPORT TYPE Final	3. DATES COVERED	
		START DATE 20210924	END DATE 20221223
4. TITLE AND SUBTITLE Multifunctional Behavior of Fe-Doped Titanate-Based High-Entropy Perovskite Oxides			
5a. CONTRACT NUMBER		5b. GRANT NUMBER FA2386-21-1-4128	5c. PROGRAM ELEMENT NUMBER
5d. PROJECT NUMBER		5e. TASK NUMBER	5f. WORK UNIT NUMBER
6. AUTHOR(S) Natthaphon Raengthon, Ketkiao Bunpang			
7. PERFORMING ORGANIZATION NAME(S) AND ADDRESS(ES) CHULALONGKORN UNIVERSITY 254 PHAYATHAI ROAD PATHUM WAN, BANGKOK 10330 THA			8. PERFORMING ORGANIZATION REPORT NUMBER
9. SPONSORING/MONITORING AGENCY NAME(S) AND ADDRESS(ES) AOARD UNIT 45002 APO AP 96338-5002		10. SPONSOR/MONITOR'S ACRONYM(S) AFRL/AFOSR IOA	11. SPONSOR/MONITOR'S REPORT NUMBER(S) AFRL-AFOSR-JP-TR-2023-0071
12. DISTRIBUTION/AVAILABILITY STATEMENT A Distribution Unlimited: PB Public Release			
13. SUPPLEMENTARY NOTES			
14. ABSTRACT High-entropy oxides have gain attention recently due to their flexibilities in formation of single-phase materials containing multiple cations, which may lead to promising properties. In this investigation, (Na _{0.2} Bi _{0.2} Ba _{0.2} Sr _{0.2} Ca _{0.2})TiO ₃ compound persisting perovskite structure is selected to further study effect of Fe substitution in Ti sublattice. Compounds prepared by solid state reaction technique exhibit single-phase cubic perovskite structure when doping with Fe < 0.5 mol. Change in lattice parameter and local structure can be observed by laboratory XRD and Raman spectrometer. Evolution of microstructure can be clearly seen. Grain size increases when small concentration of Fe is doped, however, it decreases when doped at higher concentration. Substitution of Ti by Fe, as acceptor doping, affects dielectric properties significantly. Slight decrease of dielectric permittivity at room temperature and increase in dielectric loss at high temperature are revealed as doping concentration increases. High-field dielectric response transforms from the slim and linear dielectric behavior of undoped sample to the more lossy dielectric behavior of the doped samples. M-H behavior of calcined powders exhibit similar characteristic to superparamagnetism when doped at higher concentration than 0.1 mol. Further investigation of magnetism is needed. Thus, based on this study, this compound shows promising multifunctionality where both dielectric and magnetic behavior coexists.			
15. SUBJECT TERMS			
16. SECURITY CLASSIFICATION OF:		17. LIMITATION OF ABSTRACT SAR	18. NUMBER OF PAGES 14
a. REPORT U	b. ABSTRACT U		
19a. NAME OF RESPONSIBLE PERSON TODD RUSHING		19b. PHONE NUMBER (Include area code) 315-227-7003	

Standard Form 298 (Rev. 5/2020)
Prescribed by ANSI Std. Z39.18

Characteristics of Fe-doped ($\text{Na}_{0.2}\text{Bi}_{0.2}\text{Ba}_{0.2}\text{Sr}_{0.2}\text{Ca}_{0.2}$) TiO_3 high-entropy perovskite ceramics

Ketkaeo Bunpang^{1,2}, Puripat Kantha³, Travis L. Thornell⁴, Natthaphon Raengthon^{1,2,5,*}

¹Department of Materials Science, Faculty of Science, Chulalongkorn University, Bangkok, 10330, Thailand

²Center of Excellence in Physics of Energy Materials (CE:PEM), Department of Physics, Faculty of Science, Chulalongkorn University, Bangkok, 10330, Thailand

³Division of Physics, Faculty of Science and Technology, Rajamangala University of Technology Thanyaburi, Pathum Thani, 12110, Thailand

⁴US Army Engineer Research and Development Center, Vicksburg, Mississippi, 39180 USA

⁵Center of Excellence on Advanced Materials for Energy Storage, Chulalongkorn University, Bangkok, 10330, Thailand

*Corresponding author: Natthaphon.R@chula.ac.th

Abstract

High-entropy oxides have gain attention recently due to their flexibilities in formation of single-phase materials containing multiple cations, which may lead to promising properties. In this investigation, ($\text{Na}_{0.2}\text{Bi}_{0.2}\text{Ba}_{0.2}\text{Sr}_{0.2}\text{Ca}_{0.2}$) TiO_3 compound persisting perovskite structure is selected to further study effect of Fe substitution in Ti sublattice. Compounds prepared by solid-state reaction technique exhibit single-phase cubic perovskite structure when doping with Fe < 0.5 mol. Change in lattice parameter and local structure can be observed by laboratory XRD and Raman spectrometer. Evolution of microstructure can be clearly seen. Grain size increases when small concentration of Fe is doped, however, it decreases when doped at higher concentration. Substitution of Ti by Fe, as acceptor doping, affects dielectric properties significantly. Slight decrease of dielectric permittivity at room temperature and increase in dielectric loss at high temperature are revealed as doping concentration increases. High-field dielectric response transforms from the slim and linear dielectric behavior of undoped sample to the more lossy dielectric behavior of the doped samples. M-H behavior of calcined powders exhibit similar characteristic to superparamagnetism when doped at higher concentration than 0.1 mol. Further investigation of magnetism is needed. Thus, based on this study, this compound shows promising multifunctionality where both dielectric and magnetic behavior coexists.

The content in this document has not been published. (23 March 2023)

Introduction

High-entropy oxides, also known as entropy-stabilized oxides, are a new class of materials that has gained interest recently. The concept of this material originated from high-entropy alloys where an equi-atomic multicomponent (> 5 atoms) forms a single-phase compound. According to thermodynamic parameters, the material is considered as high-entropy alloys when its' configurational entropy (ΔS_{conf}) is greater than $1.5R$ ($R =$ gas constant). The increase in configurational entropy results in lower Gibbs' free energy of the material. Therefore, the single phase is stabilized. Various structures of oxides, including rocksalt, spinel, fluorite, and perovskite, were investigated recently. They showed high potential to be utilized in many applications such as good thermal conductivity, high ionic conductivity, improved electrochemical performance for energy storage applications, and magnetic properties. Perovskite material is known as a compound with the general chemical formula of ABO_3 , where A represents cation at 12-fold coordination site, and B represents cation at 6-fold coordination site. As shown in Figure 1, the crystallographic model shows an example high-entropy perovskite oxide compound, where A-site contains 5 equi-molar cations while B-site contains only Ti ion.

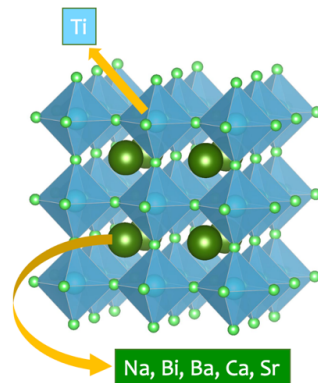


Figure 1. Crystallographic model of perovskite structure.

The $(\text{Na}_{0.2}\text{Bi}_{0.2}\text{Ba}_{0.2}\text{Ca}_{0.2}\text{Sr}_{0.2})\text{TiO}_3$ compound was investigated by Pu *et al.* and was found to stabilize as single phase with perovskite structure [1]. The disorder of A-cations generates dielectric characteristics of relaxor ferroelectric behavior with high dielectric permittivity (> 2500) at around room temperature, as shown in Figure 2. This study shows that the high-entropy perovskite oxides with proper chemical composition can provide promising electrical properties, in particular ferroelectric and dielectric behavior.

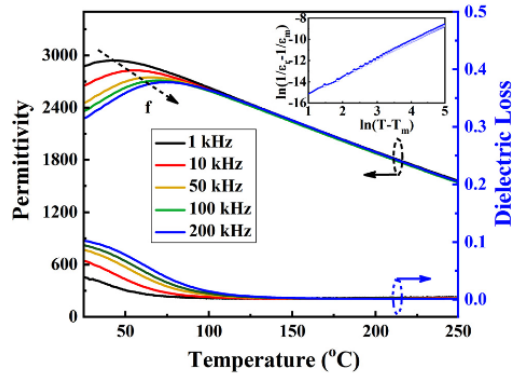


Figure 2. Dielectric properties as a function temperature of $(\text{Na}_{0.2}\text{Bi}_{0.2}\text{Ba}_{0.2}\text{Ca}_{0.2}\text{Sr}_{0.2})\text{TiO}_3$ ceramics [1].

In this study, the main goal is to explore multifunctional behavior in the high-entropy perovskite oxides. Perovskite structure is known to be versatile for doping various cations into each crystallographic site. Therefore, by doping the magnetically active cation into the B-site of the high-entropy perovskite compound, it is expected to induce multifunctionality of electric and magnetic character onto this new group of material. In particular, this study will explore effects of doping Fe-ion on multifunctionality of high-entropy perovskite $(\text{Na}_{0.2}\text{Bi}_{0.2}\text{Ba}_{0.2}\text{Ca}_{0.2}\text{Sr}_{0.2})(\text{Ti}_{1-x}\text{Fe}_x)\text{O}_3$ ceramics. In this case, the BO_6 octahedra consists of TiO_6 and FeO_6 octahedra with different ratios depending on doping concentration. It is expected that coexistence of two different cations (Ti and Fe) in BO_6 octahedral will, therefore, give rise in multifunctionality.

Experimental Procedure

The compound selected for this study is $(\text{Na}_{0.2}\text{Bi}_{0.2}\text{Ba}_{0.2}\text{Ca}_{0.2}\text{Sr}_{0.2})(\text{Ti}_{1-x}\text{Fe}_x)\text{O}_3$ (NBBST). The Fe doping concentration was varied from $x = 0$ to 0.5 with 0.1 increments, which later labelled as 0.0Fe, 0.1Fe, 0.2Fe, 0.3Fe, 0.4Fe, and 0.5Fe. Batch calculations was performed according to stoichiometry of each composition. Starting precursors of Na_2CO_3 , Bi_2O_3 , BaCO_3 , CaCO_3 , SrCO_3 , TiO_2 , and Fe_2O_3 were used in this study. Powders of each precursor was dried in an electric oven prior to weighing to eliminate adsorbed moisture. The precursors were mixed and ground by ball milling method for 24 hours using ZrO_2 milling media and ethanol as medium. Afterwards the mixture was dried in an electric oven for 24 hours. The dried powders were calcined in an electric oven at $975\text{ }^\circ\text{C}$ for 2 hours with heating and cooling rate of $5\text{ }^\circ\text{C}/\text{min}$. Single phase formation of perovskite was evaluated by X-ray diffraction (XRD) techniques for all compositions. The doping

limit was determined by observing the composition consisting of secondary phases, if occurred. The calcined powders were ground by ball milling method as described earlier to obtain reduced particle size. Ceramic samples, with a disc shape of 10 mm in diameter and 1 mm in thickness, were prepared by uniaxial pressing technique. The pressed disc samples were sintered in an electric oven at various temperatures between 1250 - 1275 °C for 2 hours with heating/cooling rate of 2 °C /min to find optimum sintering conditions. Density and shrinkage measurements were performed to observe the physical properties of the prepared ceramics. The phase purity was verified by XRD technique. The structural information of ceramic samples was investigated by Raman spectroscopy. Microstructure of the ceramic samples was observed by scanning electron microscope (SEM). For electrical properties measurements, the ceramic samples were polished its surface on both sides prior to applying a silver electrode. Dielectric permittivity and dielectric loss ($\tan \delta$) were measured as a function of frequency and temperature. The sample was mounted onto sample fixtures that withstand temperature variation. The sample was connected to LCR meter, which measures the dielectric permittivity and $\tan \delta$, and a computer to automatically collect data when frequency of measurement and temperature were varied. The ferroelectric behavior was measured by using the Ferroelectric test system. The measurement was carried out at room temperature. For magnetic properties measurements, the sample was measured by the Versalab (Quantum design, USA).

Results and Discussion

Phase formation of $(\text{Na}_{0.2}\text{Bi}_{0.2}\text{Ba}_{0.2}\text{Ca}_{0.2}\text{Sr}_{0.2})(\text{Ti}_{1-x}\text{Fe}_x)\text{O}_3$ compounds where $x = 0, 0.1, 0.2, 0.3, 0.4,$ and 0.5 were displayed in Figure 3. Formation of perovskite phase could be obtained for all compositions. For calcined powders, substitution of more than 0.2 mol of Fe onto Ti sublattice resulted in clearly visible tetragonal (T, JCPDS No. 01-070-4760) and cubic (C, JCPDS No. 00-034-0411) perovskites phase coexisting as well as presence of secondary phase (*). Sintering at higher temperature induced single phase formation of cubic high-entropy perovskite oxides when doped with Fe less than 0.5 mol, as shown in Figure 3. A change in lattice parameter of ceramics when doping concentration increased could be obtained as well as shown by shifting of XRD peaks' position. As listed in Table 1, lattice parameter, a , increased when doped with 0.1 mol of Fe, then decreased when doping concentration increased to 0.4 mol. The slight increment of lattice parameter when doping with 0.1 mol Fe ion was due to substitution of larger ionic size of Fe^{3+} (0.645 Å) onto Ti^{4+} (0.605 Å) sublattice. However, further substitution showed a decrease of lattice parameter. Additionally, the H phase observed in the 0.5Fe sintered sample matched

with hexagonal symmetry of perovskite, which commonly found in Fe-doped BaTiO₃ ceramics [2, 3]. It should be noted that the hexagonal phase induced by Fe doping of BaTiO₃ occurred when Ti sublattice was substitute by Fe of more than 0.02 mol [3]. However, based on our results, the occurrence of hexagonal phase appeared when doping with Fe of more than 0.4 mol. It could be suggested that titanate-based perovskite oxide with different A-site environment affected hexagonal phase formation when doped with Fe.

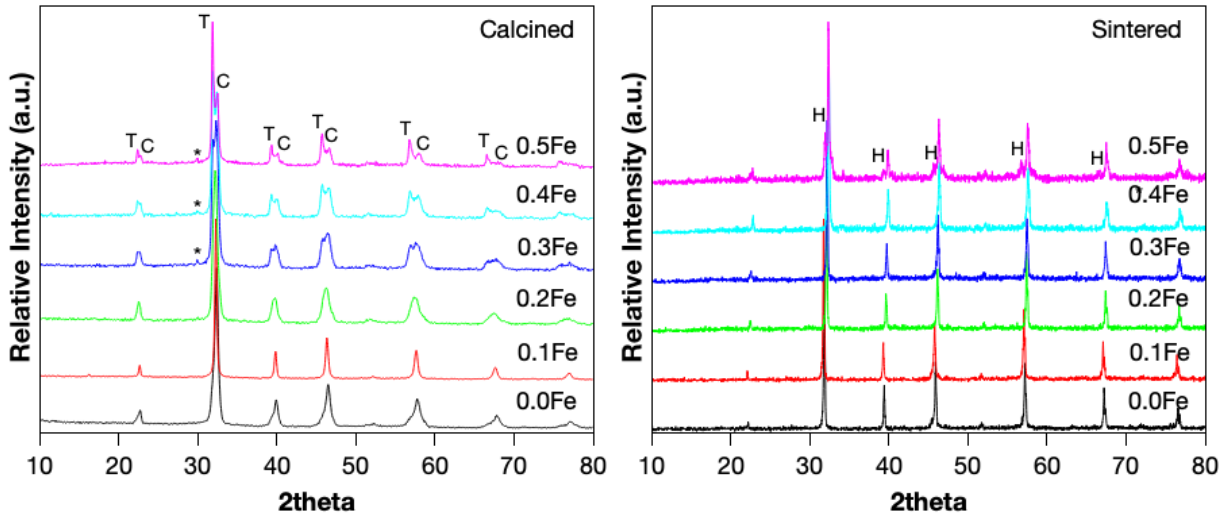


Figure 3. X-ray diffraction patterns of undoped and Fe-doped NBBSCT calcined powders and ceramics where T, C, *, H represent tetragonal perovskite, cubic perovskite, secondary phase, and hexagonal phases, respectively.

Table 1. Lattice parameter and average grain size of NBBSCT sintered ceramics.

Composition	Lattice parameter (a, Angstrom)	Average grain size (micrometer)
0.0Fe	3.9568 ± 0.0198	2.19 ± 0.12
0.1Fe	3.9662 ± 0.0240	10.36 ± 1.12
0.2Fe	3.9346 ± 0.0071	9.48 ± 1.08
0.3Fe	3.9296 ± 0.0028	2.39 ± 0.12
0.4Fe	3.9125 ± 0.0101	1.51 ± 0.06
0.5Fe	3.9173 ± 0.0072	1.02 ± 0.08

Room temperature Raman spectra of all ceramic samples were displayed in Figure 4. Broad Raman bands could be observed with characteristics aligned with ABO_3 perovskite system, similar to previously report based on $BiFeO_3 - SrTiO_3$ system [4]. In such system, multi-cations occupying at A-site could lead to overlapping of Raman modes. In general, based on $(Bi_{0.5}Na_{0.5})TiO_3$ and $BaTiO_3$ systems [5 – 11], there were three regions that should be discussed. First, the vibration of A-O bonds corresponded with spectral in the range of $100 - 200\text{ cm}^{-1}$. Second, the vibration of B-O bonds corresponded with spectral in the range of $200 - 400\text{ cm}^{-1}$. Third, the vibration modes of BO_6 octahedra corresponded with the spectral in the range of $400 - 900\text{ cm}^{-1}$. In the first region, weak and broad bands at ~ 115 and 170 cm^{-1} could be observed in high doping concentration of Fe. The slight change of these bands could be due to change in A-O vibration characteristics induced by the presence of different BO_6 surroundings, i.e., TiO_6 and FeO_6 octahedra, as well as change in unit cell. In the second region, the shifting of bands at 264 to 255 cm^{-1} could be observed when Fe doping increased. It should be noted that the 0.5Fe composition showed the broader band. Two main bands could be observed in the third region, i.e., $400 - 600\text{ cm}^{-1}$ and $600 - 900\text{ cm}^{-1}$ which directly related to vibration of BO_6 octahedra. The band at 535 cm^{-1} remained unchanged until doping concentration was higher than 0.2, then, the shift to lower wavenumber ($\sim 522\text{ cm}^{-1}$) and broader band could be observed. Additional band at 460 cm^{-1} could be clearly seen in 0.5Fe composition. Broad bands above 700 cm^{-1} transitioned to narrower bands when doping concentration increased. Similarly, the band at $\sim 650\text{ cm}^{-1}$ started to appear when Fe was higher than 0.3 mol, which became prominence at 0.5Fe composition. The significant change in Raman band characteristics in the third region, vibration of BO_6 octahedra, suggested that Fe substituted Ti sublattice leading to the coexistence of TiO_6 and FeO_6 octahedra.

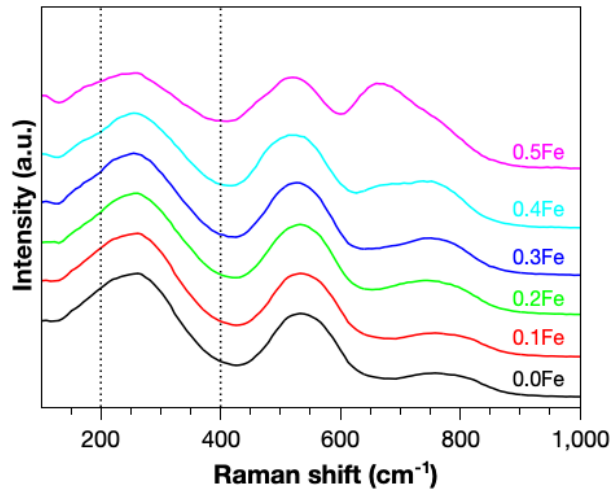


Figure 4. Raman spectra of undoped and Fe-doped NBBST ceramics

Microstructure characterized by scanning electron microscopy technique of all compositions were displayed in Figure 5. For undoped ceramic, uniform grain size with relatively sharp edge grain could be observed. The average grain size of this composition was $2.19 \pm 0.12 \mu\text{m}$. As listed in Table 1, increment of grain size was significant for 0.1Fe and 0.2Fe compositions. Large pores were visible, which might form due to accumulation of smaller pore during sintering. However, as Fe was doped with higher concentration ($x = 0.3 - 0.5$), the average grain size reduced to smaller value with uniformed size distribution. This result suggested that Fe substitution into Ti sublattice had significant effect on microstructure formation.

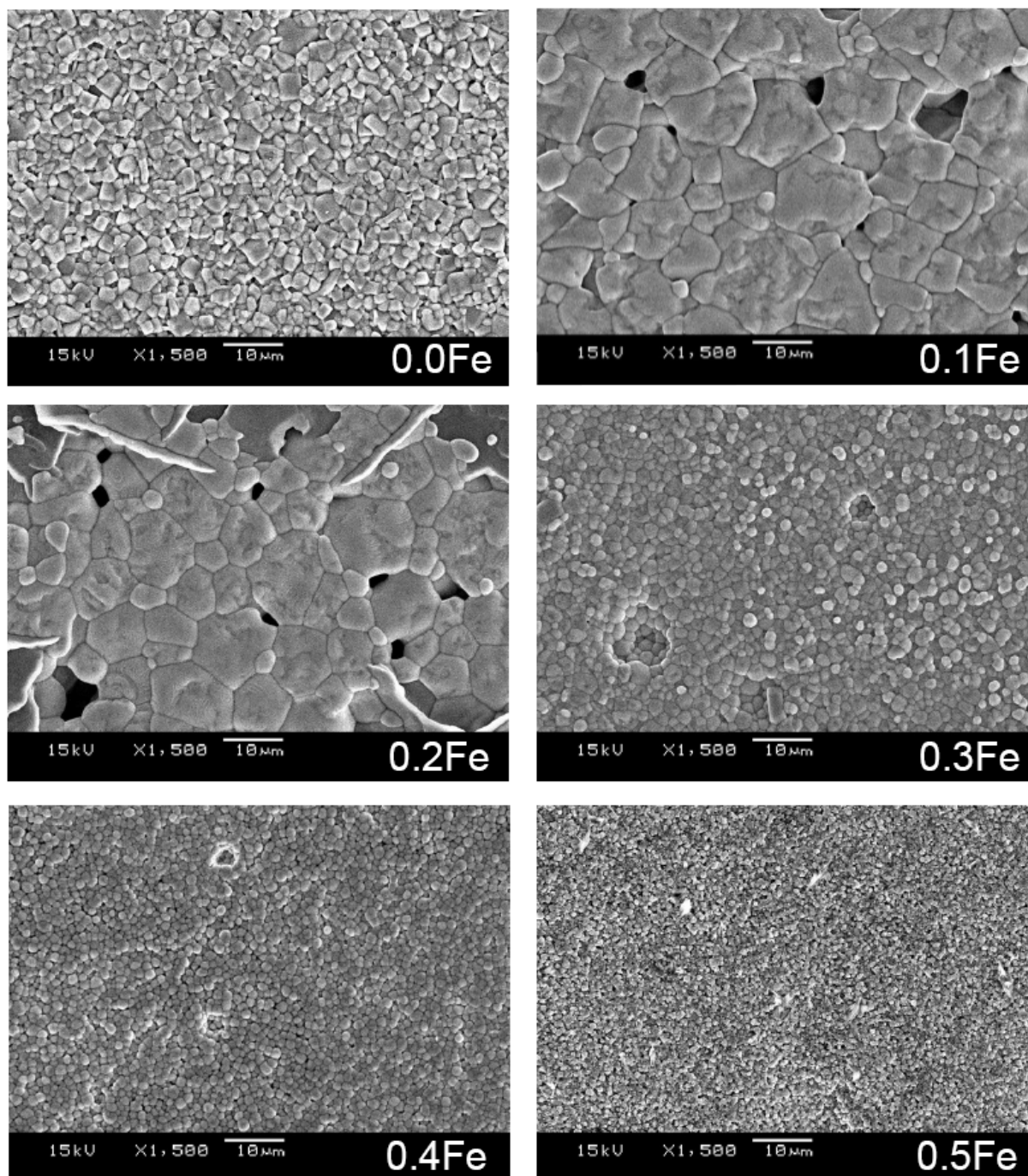
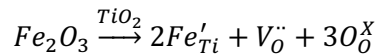


Figure 5. Microstructure of undoped and Fe-doped NBBSCT ceramics

Temperature dependence of dielectric properties of all compositions were shown in Figure 6. Relaxor ferroelectric characteristics could be observed from relative permittivity as a function of temperature and frequency of undoped sample, which T_{\max} , temperature at which relative permittivity is maximum, increased when measuring frequencies increased. This was a

characteristic of polar nanoregions (PNRs) that persisted in the materials. Relative permittivity and dielectric loss at T_{\max} , 47.7 °C, of 2859 and 0.022 were identified for this composition. Comparison of dielectric permittivity and dielectric loss were listed in Table 2. This result agreed well with previously report by Pu *et al.* [1]. Substitution of Ti sublattice by Fe ion drastically change dielectric behavior as shown in the doped samples. Shifting of T_{\max} could be observed to 135.5 and 157.6 °C for $x = 0.1$ and 0.2 compositions, respectively. Moreover, frequency dependent behavior of T_{\max} could no longer be observed. Instead, diffused phase transition behavior was seen together with high dielectric loss at high temperatures above T_{\max} . This could originate from acceptor doping that induce oxygen vacancies formation, as shown below, resulting in high dielectric loss as well as changes in microstructure.



Furthermore, as doping concentration increased, $x = 0.3 - 0.5$, the dielectric behavior became lossy where relative permittivity increased sharply as temperature increased as well as high dielectric loss over a wide range of temperatures. It should be noted that T_{\max} could not be identified, and room temperature dielectric loss increased as a function of doping concentration for $x = 0.3 - 0.5$, ranging from 0.202 to 2.150. Since the concentration of acceptor doping cation increased, the concentration of oxygen vacancies could be further induced, thus, the high dielectric loss could be observed. Therefore, acceptor doping of Fe into Ti sublattice in high-entropy NBSCT ceramics play the important role in governing dielectric properties and their temperature dependence behavior.

Table 2. Relative permittivity and dielectric loss at 1 kHz of NBSCT ceramics

Composition	ϵ_r (30 °C)	$\tan \delta$ (30 °C)	T_{\max} (°C)	ϵ_r (T_{\max})	$\tan \delta$ (T_{\max})
0.0Fe	2846	0.034	47.7	2859	0.022
0.1Fe	1009	0.011	135.5	1188	0.017
0.2Fe	896	0.013	157.6	1022	0.195
0.3Fe	1036	0.202	N/A	N/A	N/A
0.4Fe	533	0.644	N/A	N/A	N/A
0.5Fe	1606	2.150	N/A	N/A	N/A

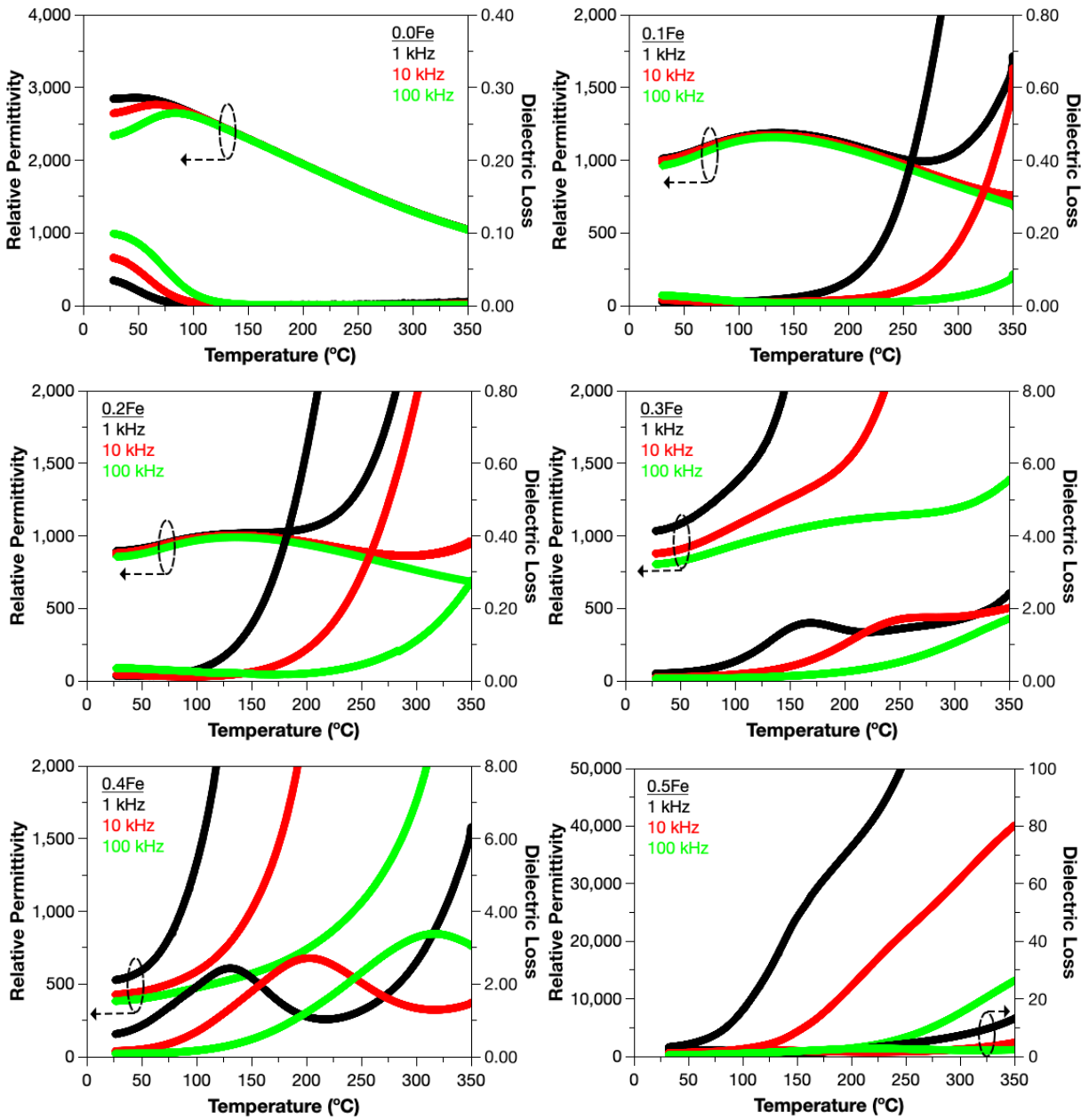


Figure 6. Temperature dependence of relative permittivity and dielectric loss of undoped and Fe-doped NBBST ceramics

Electric field dependence of polarization behavior of compositions where $x = 0.0, 0.1$ and 0.2 compositions were investigated, as shown in Figure 7. Samples with higher doping concentration ($0.3\text{Fe}, 0.4\text{Fe}$ and 0.5Fe) were not measurable since dielectric loss was high at room temperature. Hysteresis loop of the undoped sample showed a slim and linear loop under applied electric field of 30 kV/cm , persisting maximum polarization (P_{max}) and remnant polarization

(P_R) of 8.42 and 0.23 $\mu\text{C}/\text{cm}^2$, respectively. Increasing Fe doping concentration reduced P_{max} and the hysteresis loop transformed into open loop without saturation of polarization. Larger area under curve of P vs. E indicated that the sample became more lossy, which agreed with the low field dielectric behavior, i.e., magnitude of dielectric loss.

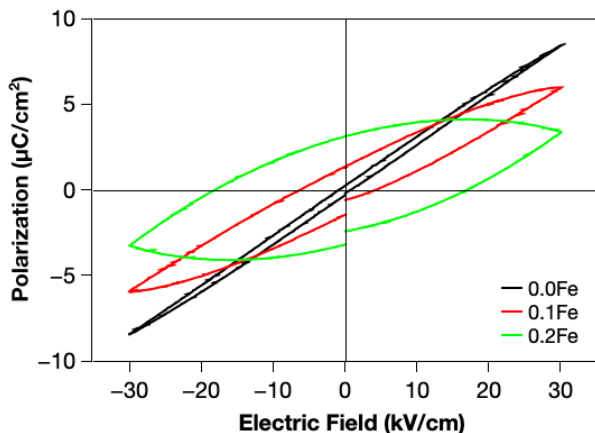


Figure 7. Room temperature ferroelectric hysteresis loops of undoped and Fe-doped NBBST ceramics

Initial investigation of room temperature magnetic response of calcine powders was conducted by using vibrating sample magnetometer, as shown in Figure 8. The M-H curve showed that for the undoped and the 0.1Fe samples exhibited linear response suggesting paramagnetic behavior. However, the nonlinear behavior of M-H curves could be observed in the $x \geq 0.2$ compositions, suggesting weak ferromagnetic or superparamagnetic behavior. Magnetization at high field, for example, at 30,000 Oersted, exhibit the following trend: $0.0\text{Fe} < 0.1\text{Fe} < 0.3\text{Fe} < 0.2\text{Fe} < 0.4\text{Fe} < 0.5\text{Fe}$. Increasing in magnetization of 0.3Fe, 0.4Fe, and 0.5Fe samples could be related to phase content. Based on XRD data shown in Figure 3, intensity of cubic phase reduced when x increased from 0.3 to 0.5. It could, therefore, stated that increasing tetragonal phase in Fe-doped samples enhanced magnetization. Further investigation of magnetic behavior of ceramic samples was needed to gain more understanding.

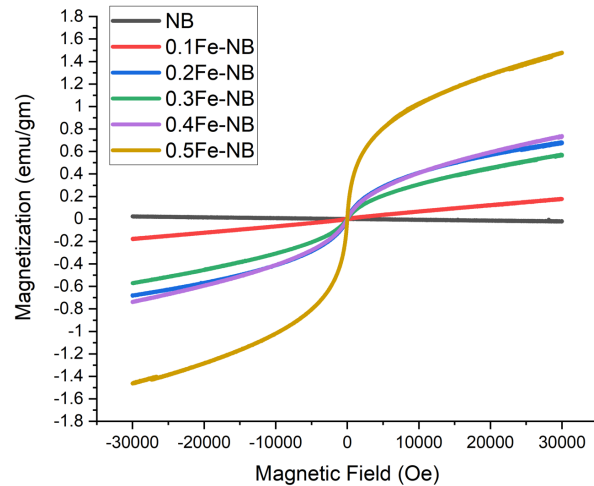


Figure 6. Room temperature magnetic hysteresis loops of undoped and Fe-doped NBBST calcined powders

Conclusions

High-entropy perovskite oxides based on $(\text{Na}_{0.2}\text{Bi}_{0.2}\text{Ba}_{0.2}\text{Sr}_{0.2}\text{Ca}_{0.2})\text{TiO}_3$ compound are selected to study the effect of Fe substitution in Ti sublattice. Compounds prepared by solid-state reaction technique exhibit single-phase perovskite with cubic structure when doped with Fe < 0.5 mol. Hexagonal perovskite phase can be observed based on XRD data when doped with 0.5 mol of Fe. Lattice parameter and local structure slightly change when doping concentration increase. Grain size increases when small concentration of Fe is doped, however, it decreases when doped at higher concentration. Acceptor doping of Fe affects dielectric properties significantly, which slight decrease of dielectric permittivity at room temperature and increase in dielectric loss at high temperature for high doping concentration. P vs. E responses transform from the slim and linear dielectric behavior of undoped sample to the more lossy dielectric behavior of the doped samples. Calcined powders exhibit similar characteristic to superparamagnetism when doped at higher concentration than 0.1 mol. Based on this study, this compound shows promising multifunctionality where both dielectric and magnetic behavior coexists, which need further investigation to fully understand their characteristics.

Acknowledgement

This material is based upon work supported by the Air Force Office of Scientific Research under award number FA2386-21-1-4128.

Reference

- [1] Y. Pu, Q. Zhang, R. Li, M. Chen., X. Du, and S. Zhou, Dielectric properties and electrocaloric effect of high-entropy $(\text{Na}_{0.2}\text{Bi}_{0.2}\text{Ba}_{0.2}\text{Sr}_{0.2}\text{Ca}_{0.2})\text{TiO}_3$ ceramic, *Appl. Phys. Lett.*, 115, 223901 (2019).
- [2] I. Mikulska, M. Valant, I. Arcon, and D. Lisjak, X-ray Absorption Spectroscopy Studies of the Room-Temperature Ferromagnetic Fe-Doped 6H-BaTiO₃, *J. Am. Ceram. Soc.*, 98[4], 1156-1161 (2015).
- [3] D. Ginting, S.C. Yu, T.L. Phan, N.V. Dang, T.D. Thanh, and V.D. Lam, Electron-Spin-Resonance Spectra and Ferroelectricity of $\text{BaTi}_{1-x}\text{Fe}_x\text{O}_3$, *J. Korean. Phys. Soc.*, 62[12], 2128-2132 (2013).
- [4] F. Yan, H. Bai, G. Ge, J. Lin, C. Shi, K. Zhu, B. Shen, J. Zhai, and S. Zhang, Composition and structure optimized BiFeO_3 - SrTiO_3 lead-free ceramics with ultrahigh energy storage performance, *Small*, 18, 2106515 (2022).
- [5] J. Kreisel, A.M. Glazer, G. Jones, P.A. Thomas, L. Abello, and G. Lucazeau, An x-ray diffraction and Raman spectroscopy investigation of A-site substituted perovskite compounds: the $(\text{Na}_{1-x}\text{K}_x)_{0.5}\text{Bi}_{0.5}\text{TiO}_3$ ($0 \leq x \leq 1$) solid solution, *J. Phys.: Condens. Matter.*, 12, 3267-3280 (2000).
- [6] Y. Mendez-Gonzalez, A. Palaiz-Barranco, A.L. Curcio, A.D. Rodrigues, and J.D.S. Guerra, Raman spectroscopy study of the la-modified $(\text{Bi}_{0.5}\text{Na}_{0.5})_{0.92}\text{Ba}_{0.08}\text{TiO}_3$ lead-free ceramic system, *J. Raman. Spectrosc.*, 50, 1044-1050 (2019).
- [7] S. Prasertpalichat, T. Siritanon, N. Nuntawong, and D.P. Cann, Structural characterization of A-site nonstoichiometric $(1-x)\text{Bi}_{0.5}\text{Na}_{0.5}\text{TiO}_3$ - $x\text{BaTiO}_3$ ceramics, *J. Mater. Sci.*, 54, 1162-1170 (2019).
- [8] K. Anjali, T.G. Ajithkumar, and P.A. Joy, Raman and ^{23}Na solid-state NMR studies on the lead-free ferroelectrics $\text{Bi}_{0.5}(\text{Na}_{1-x}\text{K}_x)_{0.5}\text{TiO}_3$ in the morphotropic phase boundary region, *Materials Research Bulletin*, 118, 110506 (2019).
- [9] S. Rajan, P.M. Mohammed Gazzali, and G. Chandrasekaran, Impact of Fe on structural modification and room temperature magnetic ordering in BaTiO_3 , *Spectrochimica Acta Part A: Molecular and Biomolecular Spectroscopy*, 171, 80-89 (2017).

- [10] J. Pokorny, U.M. Pasha, L. Ben, O.P. Thakur, D.C. Sinclair, and I.M. Reaney, Use of Raman spectroscopy to determine the site occupancy of dopants in BaTiO₃, J. Appl. Phys., 109, 114110 (2011).
- [11] V. Dwij, B.K. De, G. Sharma, D.K. Shukla, M.K. Gupta, R. Mittal, and V. Sathe, Revisiting eigen displacements of tetragonal BaTiO₃: Combined first principle and experimental investigation, Physica B, 624, 413381 (2022).